Acrylamide Quenching of the Intrinsic Fluorescence of Tryptophan Residues Genetically Engineered into the Soluble Colicin E1 Channel Peptide. Structural Characterization of the Insertion-Competent State†

A. R. Merrill,*,‡ L. R. Palmer,‡ and A. G. Szabo§

Guelph–Waterloo Centre for Graduate Work in Chemistry, Department of Chemistry and Biochemistry, University of Guelph, Guelph, Ontario, Canada N1G 2W1, and Institute for Biological Sciences, National Research Council, Ottawa, Ontario, Canada K1A 0R6

Received February 10, 1993; Revised Manuscript Received April 16, 1993

ABSTRACT: Colicin E1 or any of its COOH-terminal channel peptides can be activated *in vitro* by acidic (<4.5) pH or detergents. In its activated or insertion-competent state, the colicin E1 thermolytic (178 residue) channel peptide demonstrated an increased ability to bind and form channels in artificial membranes. An earlier report [Merrill *et al.* (1990) *Biochemistry 29*, 5829–5836] indicated that the structural change occurring in the channel peptide upon activation was not a large unfolding but seemingly involves a more subtle conformational change. To probe the solution structure of the colicin channel peptide and the structural changes occurring upon activation, 12 single-tryptophan-containing mutant peptides have been prepared. All of the peptides displayed cellular cytotoxicity comparable to the wild-type peptide. Fluorescence quenching by acrylamide of each Trp residue genetically engineered into the channel peptide indicated that tryptophyls located at positions 355, 367, 393, 413, and 443 report significant conformational changes which are associated with the insertion-competent state. Calculation of the bimolecular quenching constants for each single-Trp peptide showed that there are three classes of Trp residues found in the native colicin E1 channel peptide. None of the Trp residues were found to be completely inaccessible to acrylamide (buried). The NH_2-terminal region near Trp-355 and -367 along with the COOH-terminal hydrophobic domain, including Trp-484, -495, and -507, was largely buried in the channel peptide soluble structure. Two peptide segments, one containing Trp-393, -404, and -413 and a second encompassing Trp-431 and -443, were moderately to very exposed regions in the soluble channel peptide. Activation of the peptide to its insertion-competent state resulted in the exposure of the three N-terminal Trp residues (W-355, W-367, and W-393). In addition, W-443, located in the voltage-responsive segment of the channel peptide, became more exposed upon low-pH activation. Conversely, the Trp residue at position 413 became significantly more buried upon peptide activation.

Colicin E1 is a 522-residue polypeptide found naturally encoded by a plasmid (ColE1) which contains the *cea* (structural gene) as well as *imm* (immunity) and *kil* genes. It is lethal to *Escherichia coli* and related bacterial strains that possess the vitamin B_{12} receptor and do not carry a colicin E1-encoding plasmid or contain *tol* (tolerant) mutations affecting the cell envelope. Colicin E1 exerts its cytotoxic action by forming a channel in the cytoplasmic membrane which becomes sufficiently conductive to depolarize and deenergize the cell (Gould & Cramer, 1977; Cleveland *et al.*, 1983). The prerequisites for channel formation are binding of the colicin polypeptide to a receptor in the outer membrane and translocation across this membrane, followed by channel formation in the *E. coli* inner membrane. The molecular events associated with colicin E1 channel formation in the cytoplasmic membrane can be studied *in vitro* by using artificial planar bilayer membranes (Bullock *et al.*, 1983) and artificial membrane vesicles (Peterson & Cramer, 1987).

The colicin E1 primary sequence has been determined (Yamada *et al.*, 1982), and it can be divided into three functional segments: a translocation domain (residues 1–230), a receptor-binding domain (residues 231–370), and a channel-forming domain (residues 371–522). Active channel-forming peptides containing the carboxy-terminal (COOH-terminal)[1] one-third of the molecule can be prepared by treatment of the whole colicin with dilute protease solutions (Davidson *et al.*, 1985). The crystal structure of a soluble C-terminal channel-forming peptide of colicin A (a similar channel-forming colicin) made by thermolysin proteolysis of the intact colicin (Lazdunski *et al.*, 1988) has been determined to 2.5-Å resolution (Parker *et al.*, 1989) and later refined to 2.4 Å (Parker *et al.*, 1992). This 204-residue peptide contains 10 α-helices ranging in length from 9 to 24 residues, with an average length of 13 residues. One- and two-dimensional ^{1}H-NMR spectra of the colicin E1 thermolytic channel peptide are consistent with the structural features of the crystal for the soluble colicin A channel peptide (Wormald *et al.*, 1990). Also, the E1 channel peptide was found to be highly α-helical by circular dichroism (CD) analysis of the soluble structure (Brunden *et al.*, 1984)

† This work was supported by the Medical Research Council of Canada (A.R.M.) and the National Research Council of Canada (A.G.S.).

* Author to whom correspondence should be addressed.
‡ University of Guelph.
§ National Research Council.

[1] Abbreviations: CD, circular dichroism; COOH-terminal, carboxy terminal; DMG, 3,3-dimethylglutaric acid; FTIR, Fourier transform infrared; HPLC, high-performance liquid chromatography; k_q, bimolecular quenching constant; K_{SV}, Stern–Volmer quenching constant; λ_{em}-max, fluorescence emission wavelength maximum; MES, 2-(*N*-morpholino)ethanesulfonic acid; NATA, *N*-acetyltryptophanamide; NH_2-terminal, amino terminal; SDS–PAGE, sodium dodecyl sulfate–polyacrylamide gel electrophoresis; $\langle\tau\rangle$, intensity-weighted mean fluorescence lifetime; TRIS, tris(hydroxymethyl)aminomethane; Trp, tryptophan.

0006-2960/93/0432-6974$04.00/0

and from FTIR analysis of the membrane-bound peptide (Rath *et al.*, 1990).

The requirement of acidic pH for *in vitro* activity and the pH optimum of the channel peptide activity (pH 3.5) with artificial membrane vesicles is shared by colicin A and several other toxins such as diphtheria toxin (London, 1992). There is a pH dependence for both binding to membranes (pH_{max} 3.5; Gould & Cramer, 1977) and voltage-dependent insertion (Merrill & Cramer, 1990). Several acidic residues are apparently involved in conferring the acidic pH dependence, presumably by disrupting salt bridges at low pH. This involvement of acidic residues was deduced from the shape of the titration curve of colicin E1 activity, which corresponds to that expected for the protonation of a single ionizable group (Shiver *et al.*, 1987). Substitution of neutral residues for E-468 and D-509, both conserved acidic residues, had only a small effect on reduction of the measured pH dependence (Shiver *et al.*, 1987, 1988), indicating the involvement of acidic residues other than E-468 and D-509.

Acidic pH (<4.5) altered the structure of the C-terminal channel peptide, as indicated by increased susceptibility to proteases and enhanced accessibility of a fluorescence probe (covalently attached to C-505) to the quencher, acrylamide (Merrill *et al.*, 1990). These data suggested that the structural change may be a partial unfolding, which would be analogous to (i) protein import in mitochondria and (ii) secretion in bacteria where the translocation-competent state was inferred to be partly unfolded from an increase in protease sensitivity (Randall & Hardy, 1986). It has been suggested that the translocation-competent state at low pH might be characterized by an increase in side-chain mobility or dynamics at low pH rather than a large unfolding (Merrill *et al.*, 1990).

In an effort to probe these events occurring upon low-pH activation of a colicin E1 channel peptide, 12 single-tryptophan-containing mutants of the channel peptide were prepared by site-directed mutagenesis to take advantage of the selective spectroscopic properties of Trp. The accessibility of each Trp residue to the aqueous medium was assessed by steady-state fluorescence quenching using the nonionic quencher acrylamide (Eftink & Ghiron, 1981), and these results in combination with mean fluorescence lifetimes and wavelength emission maxima were correlated with local structural features in the peptide segment containing the Trp residue.

MATERIALS AND METHODS

Preparation of Single-Trp Mutants of Colicin E1. Single-Trp colicin E1 mutants were prepared by site-directed mutagenesis techniques as previously described (Merrill & Cramer, 1990; Song & Cramer, 1991) with a Trp residue being substituted for an endogenous Phe or Tyr at various positions in the colicin E1 protein (12 mutants). Each of the colicin mutant proteins was tested for cytotoxicity by a "spot test" on a bacterial lawn consisting of colicin-sensitive *E. coli* (strain B) cells (Song & Cramer, 1991). The *in vitro* channel-forming activity was tested for the single-Trp channel peptides as described previously (Merrill & Cramer, 1990).

Purification of Colicin E1 and Its COOH-Terminal Thermolytic Peptide. Colicin E1 was purified from *E. coli* IT3661 cells harboring the plasmid pSKE1$^-$ as described elsewhere (Song & Cramer, 1991), and the thermolytic channel peptide was isolated from a thermolytic digest of colicin E1 as described earlier (Merrill *et al.*, 1990). As a means of comparison, for some experiments the single-Trp-containing channel peptides used in fluorescence experiments were further purified by high-performance liquid chromatography (HPLC) using ion-exchange chromatography (Bio-Rad MA7S cation-exchange column, 50 × 7.8 mm). The starting buffer was 50 mM MES (Sigma), pH 6.0, and the channel peptide eluted between 150 and 200 mM NaCl. Overloading of an SDS–PAGE gel (Laemmli, 1980) with purified peptide revealed less than 1% contamination from protein impurities. Also, absorption spectra of the single-Trp mutants revealed that the protein preparations were devoid of any nonprotein contaminating chromophores.

Spectroscopic Measurements. (1) Steady-State Fluorescence Measurements. Steady-state fluorescence measurements were made on a PTI Alphascan-2 spectrofluorometer (Photon Technology Inc., South Brunswick, NJ) equipped with stirrer, thermostated cell holder, and emission correction features. Fluorescence data were obtained in the ratio mode making use of the reference cell quantum counter. Corrections were made for the signal from the appropriate blank and for the wavelength-dependent bias of the optical and detection systems.

(2) Stern–Volmer Quenching. Quenching experiments were performed using excitation at 295 nm (4-nm band-pass) with fluorescence emission monitored at 340 nm (4-nm band-pass). Aliquots of freshly prepared 5.0 M acrylamide (Bio-Rad) solution were added to a stirred and thermostated protein solution (20 °C) containing 10 mM DMG/100 mM NaCl, pH 3.5 or 6.0. The fluorescence intensities were corrected for dilution effects, and it was determined that upon excitation at 295 nm no corrections for absorptive screening were required ($\epsilon_{M,295}$, 0.25 M^{-1} cm^{-1} for acrylamide; Parker, 1968). Quenching results were plotted as the ratio of the fluorescence intensity in the absence of quencher (F_0) to the intensity in the presence of quencher (F) against quencher concentration. Some of the Stern–Volmer plots showed a tendency for slight upward curvature. Therefore, in these cases, only the linear region of the quenching curves was fit by linear regression analysis, and the calculated slope was equated to dynamic parameters according to the modified Stern–Volmer equation: $F_0/F = 1 + K_{SV}[Q]$, where K_{SV} is equal to $k_q\tau_0$ (Eftink & Ghiron, 1981). Protein concentrations were usually adjusted to provide an optical density at the excitation wavelength of less than 0.1.

(3) Time-Resolved Fluorescence Measurements. Time-resolved fluorescence measurements were performed by using the technique of time-correlated single photon counting with instrumentation described elsewhere (Willis & Szabo, 1989). The excitation source was a cavity-dumped dye laser (Spectra Physics) operating at 825 kHz with a pulse width of 15 ps. Emission, following vertically polarized excitation at 295, 300, or 305 nm, was detected (right-angle geometry) after passing through a Glan Taylor polarizer set at 55° to the vertical and a JY H10 monochromator, with a 4-nm band-pass, on a Hamamatsu 1564 U-01 microchannel plate photomultiplier. The channel width was 21.6 or 10.8 ps/channel, and data were collected in 1024 channels. The instrument response function determined from a scattering solution of glycogen was typically four channels (full width at half-maximum, 21.6 ps/channel). Each decay curve typically contained 5 × 10^5 to 1.5 × 10^6 total counts and required 3–5 min of data collection. The ratio of laser pulses to single-photon events was 100:1 or greater. A "no protein" blank was measured for each sample for the same accumulation time, and the blank counts were subtracted from the sample decay curve.

The function describing the fluorescence intensity decay following δ-function excitation is assumed to be a sum of

exponentials: $I(\lambda,t) = \sum\alpha_i(\lambda)\exp(-t/\tau_i)$ where τ_i is the decay time of the ith component and $\alpha_i(\lambda)$ is the preexponential factor at emission wavelength λ. Since this model assumes τ_i is independent of λ, decay curves taken at different emission wavelengths can be analyzed simultaneously (Knutson et al., 1983). Data were analyzed by a global least-squares iterative convolution method based on the Marquardt (1963) algorithm. The preexponential factors used to calculate the mean fluorescence lifetimes were normalized so that their sum was equal to 1.0. Adequacy of the exponential decay fitting was judged by inspection of the plots of weighted residuals and by the statistical parameters χ^2 [the reduced χ^2 (Bevington, 1969)] and SVR [the serial variance ratio (Durbin & Watson, 1971; Zuker *et al.*, 1985)].

(*4*) *Circular Dichroism Measurements.* Measurements were made with a Jasco J-600 spectrometer interfaced to a PC computer. Spectra were acquired at 20 °C with a 0.1-cm path length cuvette with a sensitivity setting of 0.05° full scale, and a time constant of 1 s. The dynode voltage of the spectrometer was not allowed to exceed 400 V. The spectra were corrected for any effects due to the buffer by subtracting the appropriate blank. The mean residue molecular weight used for the calculation of mean residue ellipticities was 110 as calculated and reported earlier (Brunden *et al.*, 1984). The revised procedure of Chen *et al.* (1974), based on the Chou and Fasman protein database, was used to analyze the secondary structure content of the thermolytic peptide. Each spectrum is the average of six individual spectra and was completed on two separate samples.

Protein Determination. The concentration of whole colicin E1 and its thermolytic channel peptide was determined spectrophotometrically using molar extinction coefficients (280 nm) of 4.195×10^4 and 3.21×10^4 M^{-1} cm^{-1}, respectively (Schwartz & Helinski, 1971; Brunden *et al.*, 1984). The molar extinction coefficients for the wild-type thermolytic peptide and the single-Trp-containing peptides were calculated from the experimental values reported for whole colicin E1 by Schwartz and Helinski (1971). These values were verified experimentally by obtaining the absorption spectra of the peptides in 0.05 M sodium phosphate at pH 7.0. Immediately, 200-μL aliquots of each of the solutions were removed and placed in acid-washed hydrolysis tubes. A known amount of norleucine (internal standard) was added to each tube, and the samples were dried, 6 N HCl was added, and the samples were hydrolyzed in vacuo for 24 h at 108 °C. The hydrolyzates were dried and dissolved in 120 μL of buffer and subjected to amino acid analysis carried out on a Beckman System Gold amino acid analyzer system (Beckman Instruments) with ninhydrin detection (Moore & Stein, 1963).

RESULTS

Location of Trp in the Various Single-Trp Channel Peptides. The amino acid sequence for the colicin E1 channel peptide (calculated MW 22 864) is shown in Figure 1. The three naturally occurring Trp residues are located at positions 424, 460, and 495. The preparation of single-Trp channel peptides, each possessing a lone Trp residue at one of the sites where the endogenous Trp are located in the wild-type peptide (W-424, W-460, and W-495), has been previously reported (Merrill & Cramer, 1990). Subsequently, the number of single-Trp channel peptides has been expanded to 12. The additional sites in the COOH-terminal channel peptide where a lone Trp residue has been inserted into the protein sequence in place of either a Tyr or a Phe residue are indicated. This approach allows a mapping of the peptide conformation using

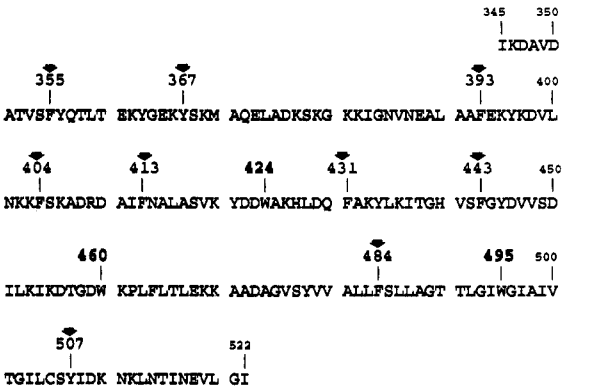

FIGURE 1: Colicin E1 thermolytic peptide amino acid sequence using the single-letter code and numbering system according to Yamada *et al.* (1982). The three naturally occurring Trp residues are indicated by the corresponding sequence position number (boldface); the positions of replacement (side-directed mutagenesis) of a Tyr or Phe with a Trp residue are indicated by an arrow (↓).

Trp as intrinsic probe. There are only two large gaps where no endogenous Tyr or Phe exists, hence not making it feasible to conduct an aromatic for aromatic residue substitution (highly conservative); these peptide segments include the region from 367 to 393 and from 460 to 484.

Structural and Functional Integrity of Single-Trp Channel Peptides. Importantly, all of the single-Trp mutant proteins possessed levels of cytotoxicity comparable to the wild-type peptide (complete clearing of a spot on a lawn of *E. coli* B5 cells at 50 ng/mL colicin E1 added as a 5-μL spot). It has been established that cytotoxicity is a sensitive measure of colicin E1 structure and function because contained within the overall cytotoxic mechanism are three specific steps (cell binding, translocation across the *E. coli* outer membrane, and channel formation in the cytoplasmic membrane). If any part of the cytotoxic mechanism is impaired by structural perturbation of the colicin molecule, it will be detected by a reduction in the toxicity of the protein (Schwartz & Helinski, 1971; Song & Cramer, 1991).

The circular dichroism (CD) spectra of the COOH-terminal tryptic fragment of colicin E1 had previously been reported (Brunden *et al.*, 1984) in aqueous solution at pH 3.5, 4.5, and 6.5. Figure 2 illustrates the far-UV CD spectrum of a slightly shorter COOH-terminal peptide of colicin E1, the 178-residue thermolytic peptide. In addition, the CD spectrum for each single-Trp thermolytic channel peptide was determined. The CD spectra of W-460 and W-507 are shown in Figure 2 as a means of comparison with the spectrum for the wild-type peptide. The CD spectra of the two single-Trp peptides were representative of those spectra obtained for all of the single-Trp channel peptides except W-404, which showed a slightly lower amount of α-helical content. The α-helical content, determined by the revised method of Chen *et al.* (1974), was 49 ± 4% for all the peptides, including the wild-type. This value was 7–8% higher than that previously reported for the tryptic peptide (41–42% α-helix; Brunden *et al.*, 1984). This discrepancy may be explained on the basis that Brunden *et al.* (1984) reported the α-helical content for a slightly larger peptide (tryptic fragment, 187 residues). Also, Brunden *et al.* used the modified method of Provencher and Glockner (1981) to fit their CD data, and the nature of the database used can have slight effects on the calculated amount of secondary structure.

Fluorescence Decay Parameters. The fluorescence decay behavior and the effect of pH on the decay parameters were

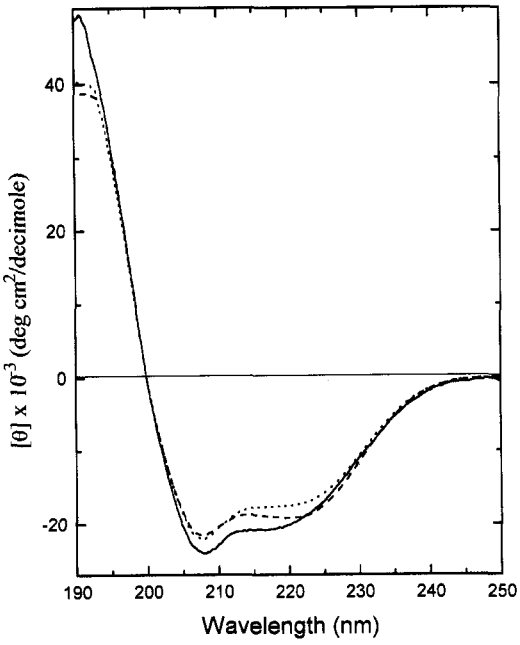

FIGURE 2: Circular dichroism spectra of the wild-type (—), W-460 (- - -), and W-507 (···) channel peptides of colicin E1. Concentrated solutions of the various peptides were diluted into 100 mM sodium fluoride/10 mM sodium phosphate buffer, pH 7.0, and run as described under Materials and Methods. Protein concentrations were between 0.1 and 0.2 mg/mL.

found to be different for each of the Trp mutants. The values in parentheses in Table I give the number of decay components for each Trp mutant. A detailed summary of the fluorescence decay parameters and their correlation with channel peptide structure will be the subject of another report. The different behavior of the time-resolved fluorescence properties of the mutants is illustrated in the parameters obtained for W-413 and W-355. The fluorescence of W-413 had two decay components at each pH. At pH 3.5, the decay times were 5.01 and 1.41 ns with normalized preexponential values of 0.67 and 0.33, respectively. At pH 6.0, the decay times were 4.67 and 1.51 ns, with the preexponential terms having values of 0.36 and 0.64, respectively. The difference in the long decay time value indicates a small change in the local interactions of the Trp residue. The dramatic reversal in the normalized preexponential terms with pH indicates a significant change in the conformation of the Trp side chain. It is noteworthy that W-413 also showed the greatest change in fluorescence emission maximum with pH (Figure 3A).

The fluorescence of Trp-355 in mutant W-355 decayed with triple-exponential decay kinetics at both pH values. At pH 3.5, the decay times were 4.33, 1.70, and 0.35 ns, and at pH 6.0, they hardly changed, having values of 4.53, 1.85, and 0.42 ns. The preexponential terms were identical at both pH values, being 0.16, 0.39, and 0.45, respectively. These parameters indicate that there was not a large pH-dependent change in the secondary or tertiary structure of the channel peptide in the immediate segment adjacent to W-355 (Willis & Szabo, 1992).

Table I displays the results of the measured mean fluorescence lifetimes ($\langle\tau\rangle$) for each of the single-Trp channel peptides. The fluorescence lifetimes were measured for each peptide at pH 6.0 (inactive conformation) and pH 3.5 (insertion-competent structure). The intensity-weighted mean fluorescence lifetimes were calculated from the individual lifetime components and the corresponding normalized preexponentials as described (see Materials and Methods; Table I legend). The $\langle\tau\rangle$ values for the single-Trp mutants can be

Table I: Tryptophan Fluorescence Parameters for Colicin E1 Single-Tryptophan Peptides

protein	pH	$\langle\tau\rangle$ (ns)[a]	λ_{em}max (nm)[b]
wild-type	3.5	4.10 (3)	323
	6.0	3.96 (3)	323
W-355	3.5	2.74 (3)	329
	6.0	2.87 (3)	329
W-367	3.5	3.43 (2)	320
	6.0	3.18 (2)	319
W-393	3.5	3.83 (2)	332
	6.0	3.30 (3)	333
W-404	3.5	4.14 (3)	337
	6.0	3.97 (3)	337
W-413	3.5	4.57 (2)	327
	6.0	3.52 (2)	332
W-424	3.5	4.62 (2)	325
	6.0	4.72 (2)	324
W-431	3.5	5.43 (2)	334
	6.0	5.34 (3)	333
W-443	3.5	2.79 (3)	338
	6.0	2.95 (3)	338
W-460	3.5	4.01 (2)	321
	6.0	4.35 (2)	323
W-484	3.5	4.21 (2)	325
	6.0	4.26 (2)	325
W-495	3.5	4.58 (2)	324
	6.0	4.72 (2)	324
W-507	3.5	2.74 (3)	324
	6.0	2.81 (3)	324
NATA	3.5	3.03 (3)	350
	6.0	3.03 (3)	350

[a] Fluorescence decay parameters were obtained from a global analysis of all datasets measured at different emission wavelengths. The individual fluorescence lifetime values, τ, and the normalized preexponential values, α, were used to calculate $\langle\tau\rangle$ values where $\langle\tau\rangle = \sum\alpha_i\tau_i^2/\sum\alpha_i\tau_i$ at 340 nm. The numbers in parentheses correspond to the number of exponential components (τ) needed to describe the fluorescence decay. Errors for each of the mean fluorescence lifetimes were all less than 5%. [b] The fluorescence spectra were obtained with λ_{ex} = 295 nm (excitation and emission slit, 2 nm), a temperature of 20 °C, and a buffer consisting of 10 mM DMG/100 mM NaCl, pH 3.5 and 6.0, and were corrected for λ-dependent bias of the emission monochromator and detector system.

categorized as those with short mean lifetimes (2–3 ns) which includes (at both pH values) the single-Trp peptides W-355, W-443, and W-507. Additionally, peptides W-367, W-393, W-404, and W-413 and the wild-type (the latter three peptides at pH 6.0 only) all have relatively short mean fluorescence lifetimes ($\langle\tau\rangle$, 3.0–4.0 ns). Single-Trp peptides, W-424, W-460, W-484, and W-495, have $\langle\tau\rangle$ values between 4.0 and 5.0 ns. This group also includes at pH 3.5 the wild-type peptide (4.10 ns), W-404 (4.14 ns), and W-413 (4.57 ns). The only single-Trp peptide with a mean fluorescence lifetime longer than 5.0 ns was W-431 (5.43 and 5.34 ns for pH 3.5 and 6.0, respectively).

Fluorescence Emission Maxima ($\lambda_{em}max$). A measure of the polarity of the environment of the Trp residue in proteins is the λ_{em}max (Creed, 1984). Table I lists the values for the λ_{em}max of the corrected fluorescence emission spectra for the wild-type and the single-Trp channel peptides. These values range from 319 nm (W-367, pH 6.0) to 338 nm (W-443, pH 3.5 and 6.0). The λ_{em}max for the free indole chromophore in aqueous solution was 350 nm [Table I; NATA (*N*-acetyltryptophanamide), pH 3.5 and 6.0]. For NATA, the λ_{em}max was independent of pH in the normal pH range. Thus, observed wavelength shifts must be indicative of pH-induced conformational changes of the Trp residue which occurred upon activation of the channel peptide soluble structure. The three Trp residues located in the hydrophobic anchor region of the channel peptide, W-484, W-495, and W-507, all have blue-shifted fluorescence emission maxima (324–325 nm for pH 3.5 and 6.0). The Trp located at positions 404 and 443

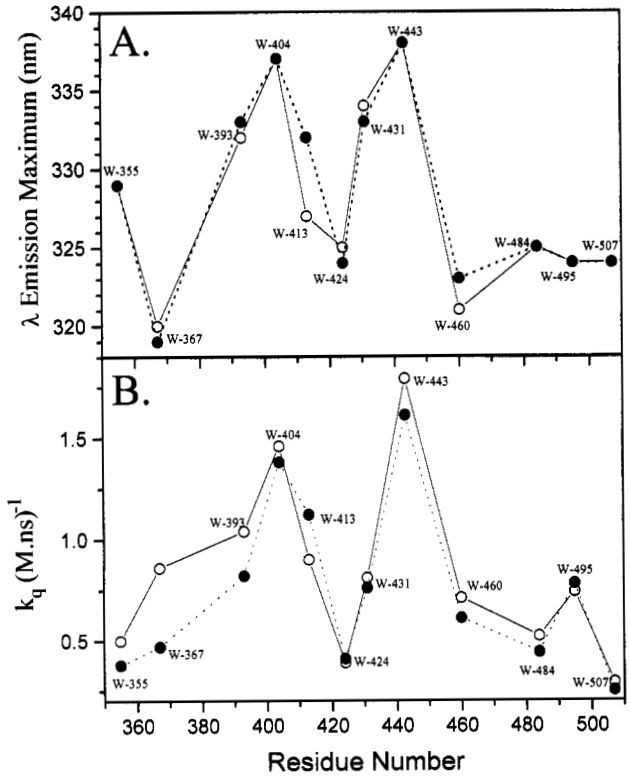

FIGURE 3: (A) Dependence of Trp residue position on the Trp fluorescence emission maximum. The fluoresence emission maxima are plotted for Trp residues in the channel peptide at pH 3.5 (○) and pH 6.0 (●). (B) Dependence of Trp sequence position on k_q. The k_q values from Table II are plotted for each Trp residue in the channel peptide at pH 3.5 (○) and pH 6.0 (●).

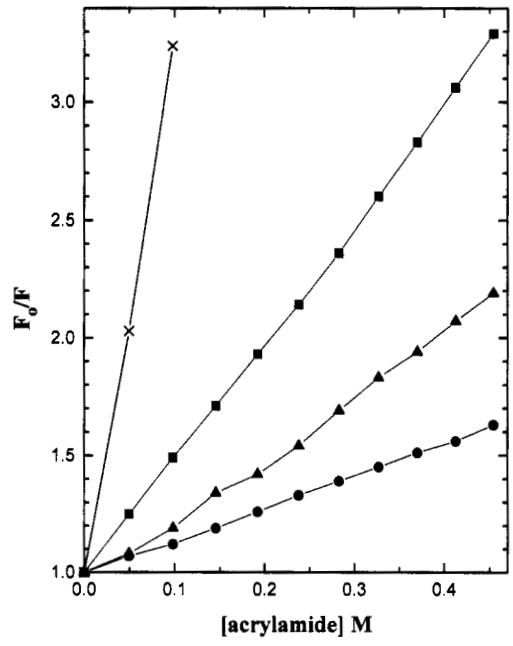

FIGURE 4: Stern–Volmer plots of Trp fluorescence quenching by acrylamide at pH 3.5. Quenching experiments were conducted as described under Materials and Methods. The single-Trp peptides were in 100 mM NaCl and 10 mM DMG buffer, pH 3.5, at 20 °C. Excitation λ, 295 nm; emission λ, 340 nm; excitation and emission slits, 4 nm. W-355 (●); W-443 (■); W-460 (▲); NATA (×).

possessed the most red-shifted fluorescence emission maxima of the Trp in the soluble channel peptide (λ_{em}max, 337 and 338 nm, respectively). The Trp residue with the highest energy fluorescence was W-367 (λ_{em}max, 319 nm). The only Trp that underwent a significant wavelength shift of its fluorescence emission upon peptide activation was W-413 which exhibited a 5-nm blue-shift (332 → 327 nm) upon acidification of the solution.

Figure 3A shows the relationship between Trp λ_{em}max and sequence position of the Trp in the channel peptide. The N-terminal region of the peptide, including Trp residues located at 355 and 367, possesses λ_{em}max values indicative of moderately buried Trp residues, with Trp-367 exhibiting the most blue-shifted fluorescence (320 and 319 nm for pH 3.5 and 6.0, respectively). Peptide segments from 393 to 413 and from 431 to 443 contain Trp residues with more red-shifted fluorescence emission maxima (327–338 nm), indicating that these Trp residues are located in relatively polar environments, possibly near the surface of the soluble peptide. In contrast, the peptide segment from Trp-460 through Trp-507 contains Trp residues with emission maxima characteristic of Trp in a more nonpolar environment (λ_{em}max, 321–325 nm).

Acrylamide Quenching of Single-Trp Mutants. The Stern–Volmer quenching plots for the titration of three single-Trp channel peptides with the nonionic quencher acrylamide are shown in Figure 4. Some of the Stern–Volmer plots showed a slight upward curvature. This upward curvature can be due to an increase in local acrylamide concentration in the vicinity of the Trp, leading to a more efficient quenching process than would normally occur due to diffusional quenching. The linear regions of the titration curves (0–0.3 M acrylamide) were best fit by linear regression analysis ($0.989 < r < 0.999$ for the K_{SV} values of all the mutants at both pH values).

It is clear from the data in Table II that consideration of the K_{SV} values by themselves can be misleading. This is because the decay time parameters of each of the Trp mutants vary. Only an estimation of the k_q from the values of K_{SV} provides a basis for describing the relative accessibility of the Trp residues. However, in most cases, the Trp fluorescence exhibited multiexponential decay behavior, as discussed earlier. The various values of k_q were calculated from the measured linear slope, $K_{SV} = k_q\tau$, using the intensity-weighted decay time $\langle\tau\rangle$, where $\langle\tau\rangle = \sum\alpha_i\tau_i^2/\sum\alpha_i\tau_i$. This value of $\langle\tau\rangle$ was considered to be the appropriate mean decay time, since the quenching curves were determined from fluorescence intensity measurements (Laws & Contino, 1992). An example of how the consideration of only K_{SV} values can be misleading is seen in the data for the W-413 mutant (Table II).

In order to correctly determine whether or not quenching over the entire acrylamide concentration range is collisional, one should measure the fluorescence decay at every acrylamide concentration. Considering the large number of single-Trp mutants which were involved in this study, this approach was not practical. However, some information on the type of quenching was obtained from a temperature study of the Stern–Volmer plots. The dominant form of fluorescence quenching for the Trp–acrylamide fluorophore–quencher pair was collisional-based on Stern–Volmer plots at various temperatures (data not shown). The effect of temperature was to increase the extent of Trp fluorescence quenching by acrylamide, which is that expected from a collisional quenching mechanism; the exact opposite was expected if the dominant quenching mechanism was static in nature.

Titration of NATA with acrylamide revealed that when the indole chromophore is free in solution the extent of quenching was large and pH independent (Figure 4, Table II; K_{SV} and k_q values ≈25 M^{-1} and 8–8.5 M^{-1} ns^{-1}, respectively). This k_q value for the quenching of NATA by acrylamide is close to the value reported by Calhoun *et al.* (1986, $k_q \approx 9$ M^{-1} ns^{-1}). The k_q values (Table II) for acrylamide quenching

Table II: Acrylamide Quenching Parameters of Tryptophan Fluorescence in Colicin E1 Single-Tryptophan Peptides

protein	pH	K_{SV} (M^{-1})[a]	K_{SV}^{-1} (M)[b]	k_q ($M \cdot ns$)$^{-1}$ [c]	class[d]
wild-type	3.5	3.13 ± 0.06	0.32	0.76 ± 0.03	2
	6.0	3.13 ± 0.04	0.32	0.79 ± 0.03	2
W-355	3.5	1.39 ± 0.04	0.72	0.50 ± 0.03	3
	6.0	1.10 ± 0.07	0.99	0.38 ± 0.05	3
W-367	3.5	2.95 ± 0.26	0.34	0.86 ± 0.08	2
	6.0	1.52 ± 0.10	0.66	0.47 ± 0.06	3
W-393	3.5	4.00 ± 0.08	0.25	1.04 ± 0.07	2
	6.0	2.72 ± 0.07	0.37	0.82 ± 0.06	2
W-404	3.5	6.06 ± 0.17	0.17	1.46 ± 0.06	2
	6.0	5.46 ± 0.13	0.18	1.38 ± 0.05	2
W-413	3.5	4.13 ± 0.09	0.24	0.90 ± 0.05	2
	6.0	4.01 ± 0.08	0.25	1.14 ± 0.05	2
W-424	3.5	1.80 ± 0.07	0.56	0.39 ± 0.03	3
	6.0	1.92 ± 0.08	0.52	0.41 ± 0.03	3
W-431	3.5	4.39 ± 0.13	0.23	0.81 ± 0.08	2
	6.0	4.08 ± 0.11	0.25	0.76 ± 0.04	2
W-443	3.5	4.99 ± 0.09	0.20	1.79 ± 0.09	1
	6.0	4.75 ± 0.08	0.21	1.61 ± 0.05	1
W-460	3.5	2.86 ± 0.08	0.35	0.71 ± 0.04	2
	6.0	2.65 ± 0.07	0.38	0.61 ± 0.03	2
W-484	3.5	2.20 ± 0.05	0.46	0.52 ± 0.03	3
	6.0	1.86 ± 0.06	0.54	0.44 ± 0.02	3
W-495	3.5	3.39 ± 0.11	0.30	0.74 ± 0.08	2
	6.0	3.69 ± 0.07	0.27	0.78 ± 0.07	2
W-507	3.5	0.81 ± 0.08	1.24	0.29 ± 0.03	3
	6.0	0.70 ± 0.07	1.43	0.25 ± 0.02	3
NATA	3.5	24.85 ± 1.21	0.040	8.20 ± 0.40	exposed
	6.0	25.76 ± 1.22	0.039	8.50 ± 0.41	exposed

[a] These values are the Stern–Volmer quenching constants obtained from the slopes of the lines for the plots of $F_0/F = 1 + K_{SV}[Q]$. Errors are the standard deviation from three to four independent experiments. [b] The inverse of the Stern–Volmer quenching constant is the [quencher] that will quench 50% of the fluorescence. [c] k_q is the bimolecular quenching constant for the acrylamide/Trp (quencher/fluorophore) pair. This quenching constant is determined from the relationship $K_{SV} = k_q\tau_0$. Errors are the standard deviation of three to four independent experiments. [d] The classification of the degree of exposure is according to Calhoun *et al.* (1986) with a slight modification. The Trp residues are classified as (1) exposed to solvent ($1.5 < k_q < 5$), (2) moderately exposed ($0.6 < k_q < 1.5$), (3) moderately buried ($0.2 < k_q < 0.6$), and (4) buried ($k_q < 0.2$). The units are M^{-1} ns^{-1}.

of Trp for the single-Trp colicin E1 channel peptides range from 0.25 to 1.79 M^{-1} ns^{-1}. This indicated that even for the most accessible Trp in the channel peptide, W-443 (k_q, 1.6–1.8 M^{-1} ns^{-1}), the indole ring was still largely excluded from the aqueous medium. The inverse of the K_{SV} values (K_{SV}^{-1}) corresponds to the concentration of acrylamide required to quench 50% of the fluorescence, and these values are also shown in Table II.

Table II displays the bimolecular quenching constant (k_q) for each of the single-Trp channel peptides (12 single-Trp-containing peptides) along with the wild-type peptide. On the basis of these results obtained from acrylamide quenching of Trp in the peptides, the individual Trp residues in the channel peptide were placed into three categories according to the grouping suggested by Calhoun *et al.* (1986). These categories include exposed, moderately exposed, and moderately buried Trp residues in proteins. W-443 was the only Trp in the channel peptide that could be classified as a surface-exposed (class 1) Trp residue, although W-404 was also readily solvent-accessible ($k_q \approx 1.40$–1.50 M^{-1} ns^{-1}). The Trp residues located at positions 393, 404, 413, 431, 460, and 495 were moderately exposed Trp (class 2) in both conformational states of the peptide. Peptides W-355, W-424, W-484, and W-507 each possessed a moderately buried Trp (class 3) residue regardless of whether the peptide had been activated or not. Trp-367 underwent a transition from a moderately buried to a moderately exposed Trp upon activation to the insertion-competent state. In contrast, Trp at residue 413 became significantly more buried upon low-pH activation of the channel peptide (k_q values, 1.14 and 0.90 M^{-1} ns^{-1} for pH 6.0 and 3.5, respectively).

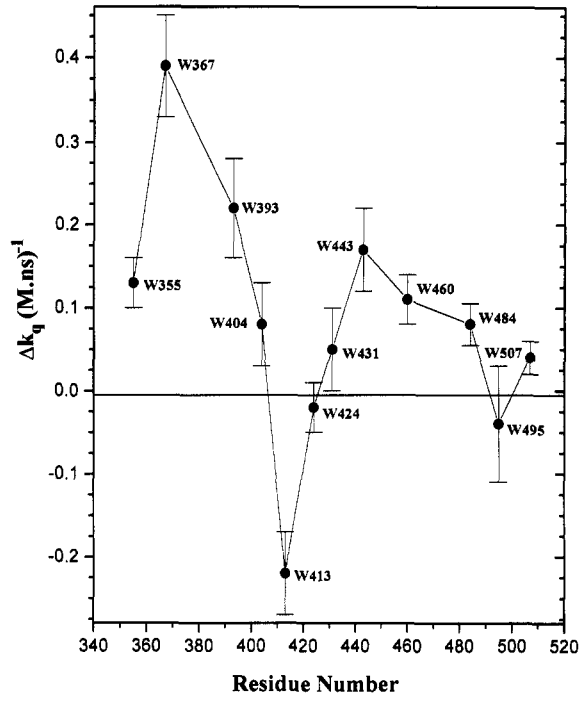

FIGURE 5: Effect of peptide activation on Trp residue exposure. The Δk_q was calculated according to the following: $\Delta k_q = k_q$(pH 3.5) – k_q(pH 6.0) (see Table II for k_q values).

Figure 3B shows the relationship between k_q and Trp location in the colicin channel peptide sequence. The overall shape and inflection points of this plot are strikingly similar to Figure 3A (above) where the λ_{em}max is also plotted against Trp position in the peptide sequence. These data indicated that similar to conclusions based on the λ_{em}max values, the N-terminal segment containing Trp-355 and -367 was largely excluded from the solvent (moderately buried). Also, the segment containing Trp-424 and -431 and the COOH-terminal segment, including Trp-460 through Trp-507, are largely inaccessible to quencher and are likely moderately buried regions of the channel peptide. Conversely, peptide segments including Trp-393, -404, and -413 and also the segment containing Trp-443 are moderate to very exposed regions in the soluble channel peptide. The shape of the curves in both Figure 3A and Figure 3B had similar features except for a slight discrepancy between the extent of solvent exposure for Trp-367 (pH 3.5) and -431 (both pH values). The quenching data indicated that the latter residue was not very solvent-exposed (moderately buried) whereas the λ_{em}max data suggest that this residue was in quite a polar environment. Also, the acrylamide quenching data indicated that W-367 upon low-pH activation became more exposed while the λ_{em}max did not change appreciably. A possible explanation for this divergence, in the case of W-431, may be that Trp-431 is in a polar environment owing to neighboring charged and/or polar amino acid residues in the peptide's tertiary structure. In the case of W-367, it may be that the polarity of its environment does not change upon low-pH activation of the channel peptide but only the extent of solvent exposure is altered.

Activation to the Insertion-Competent State. Careful inspection of the values calculated for the bimolecular quenching constants (k_q, Table II, Figure 5) reveals that several of the Trp in the colicin channel peptide became significantly

more exposed upon low-pH activation. These include Trp residues found at positions 355, 367, 393, and 443. The only Trp residue which became significantly more buried upon peptide activation was Trp-413 in the channel peptide sequence. Seven of the Trp residues showed no or only slightly significant changes in the degree of exposure upon acidification; these were W-404, W-424, W-431, W-460, W-484, W-495, and W-507.

Activation of the colicin channel peptide to the insertion-competent state increased the overall degree of exposure of the N-terminal region of the peptide (Figures 3B and 5) to the aqueous medium. The COOH-terminal one-third of the channel peptide, which includes the hydrophobic segment (A-474 to I-508), also showed a small structural change (increased solvent exposure) upon low-pH activation.

DISCUSSION

The complement of single-Trp-containing channel peptides of colicin E1 described herein has been purified and characterized and as such provides extremely useful probes of the structure and dynamics of the colicin E1 channel peptide. The Trp chromophore is sensitive to the nature of its immediate chemical environment due to its large dipole moment change upon excitation (Burstein, 1974), and has been shown to be a useful probe of protein structure and dynamics. Each of the dozen mutants isolated was shown to be active as measured by its ability to clear a lawn of sensitive *E. coli* cells and from its ability to form active channels in artificial membrane vesicles (Merrill & Cramer, 1990; data not shown). Also, the CD spectra of the wild-type and the single-Trp channel peptides were very similar, indicative of no large perturbation of the secondary structure of the mutant peptides upon replacement and insertion of Trp residues in various sites within the channel peptide sequence (Figure 2).

The Trp residue located at position 443 in the channel peptide amino acid sequence had all the characteristics of a Trp in a polar environment such as would occur in a surface-exposed residue. It had the most red-shifted fluorescence emission maximum (338 nm), the highest bimolecular quenching constant (1.60–1.80 M^{-1} ns^{-1}, Table II), and a short mean lifetime (2.8–3.0 ns, Table I). W-404 had similar characteristics which suggested that it too was surface-exposed in the soluble peptide structure [337 nm, 1.4–1.5 M^{-1} ns^{-1}, but higher $\langle\tau\rangle$ values (4.0–4.1 ns)]. Secondary structure analysis of the colicin E1 channel peptide primary sequence also indicates that W-443 and W-404 are most likely located in turn regions, hence at or near the surface of the soluble channel structure (data not shown). Accordingly, Trp residues 393, 404, 413, 460, and 495 are expected to be moderately exposed Trp residues in the soluble channel structure (k_q, 0.61–1.46 M^{-1} ns^{-1}; λ_{em}max, 321–337 nm; $\langle\tau\rangle$, 3.30–5.43 ns). Also, W-367 has the characteristics of being moderately surface-exposed in the soluble peptide structure at pH 3.5 (λ_{em}max, 320 nm; k_q, 0.86 M^{-1} ns^{-1}; $\langle\tau\rangle$, 3.43 ns).

Furthermore, considering these criteria, W-355, W-424, W-484, and W-507 are predicted to be moderately buried residues in the soluble channel peptide structure. Trp-355 possessed a λ_{em}max (329 nm) and a bimolecular quenching constant (0.38–0.50 M^{-1} ns^{-1}) characteristic of a moderately buried Trp residue in the channel peptide structure. However, Trp-355 had a mean fluorescence lifetime characteristic of an extensive deactivation mechanism occurring in the soluble structure ($\langle\tau\rangle$, 2.70–2.90 ns). Upon low-pH activation, Trp-355 became more exposed (Δk_q, 0.12 M^{-1} ns^{-1}) with no detectable change in the λ_{em}max or $\langle\tau\rangle$. Since the λ_{em}max and k_q indicate that the quenching was not caused by water, it must be that this Trp residue is in close proximity to a charged residue which promotes nonradiative deactivation of the excited state.

Trp-507 appears to be in a unique chemical environment in the channel peptide structure. The k_q values for both pH forms of the peptide were characteristic of a largely buried Trp residue (0.29 and 0.25 M^{-1} ns^{-1} for pH 3.5 and 6.0, respectively). In addition, this Trp residue had a blue-shifted λ_{em}max (324 nm for both pH forms) indicating that Trp-507 is in a relatively nonpolar environment. However, the mean fluorescence lifetimes for this Trp in the channel peptide were short (2.74 and 2.81 ns for pH 3.5 and 6.0, respectively), indicative of a significant quenching mechanism occurring in the peptide. It is interesting to note that Trp-507 is located only two residues from the single cysteine (C-505) in the channel peptide. The short mean fluorescence lifetime for Trp-507 likely reflects its close promixity to this cysteine since free sulfhydryls in proteins are known to be excellent quenchers of Trp fluorescence (Permyakov, 1993).

It was previously demonstrated that the colicin E1 channel peptide undergoes a transition upon low-pH activation from its inactive structure to an insertion-competent conformation (Merrill *et al.*, 1990). This activated "intermediate" structure was shown to possess striking similarities to the "molten-globule" folding–unfolding intermediate originally described by Ptitsyn (1987) and now widely accepted. Goot *et al.* (1991) recently proposed a similar mechanism involved in the activation of the colicin A channel peptide. Merrill *et al.* (1990) characterized the insertion-competent state of the colicin E1 channel peptide as a structure which possessed (i) increased susceptibility to protease, (ii) greater overall hydrophobicity as determined by its enhanced ability to partition into Triton X-114, and (iii) greater exposure of C-505 as monitored by the fluorescence reporter, AEDANS, covalently attached to this cysteine residue but (iv) with no significant increase in the hydrodynamic radius of the molecule (22.5 and 22.0 Å for the native and activated structures, respectively).

Changes in the Trp λ_{em}max upon peptide activation were generally not large and were localized to only a few of the Trp residues in the channel peptide. The most significant shift in the Trp λ_{em}max occurred in Trp-413 where a 5-nm blue-shift was observed upon low-pH activation, which correlated well with the concomitant decrease in the k_q value (from 1.14 M^{-1} ns^{-1}, pH 6.0, to 0.90 M^{-1} ns^{-1}, pH 3.5). Activation of the channel peptide solution structure to the insertion-competent state leads to conformational changes in the soluble structure at the amino terminus, Trp residues at positions 355, 367, and 393. There was a small increase in exposure of the COOH-terminal end of the channel peptide near W-460 and W-484. These data are consistent with previous results which suggest that activation of the solution structure of the channel peptide is not a large unfolding but rather a loosening of the native structure (Merrill *et al.*, 1990).

Fluorescence quenching of the Trp residue in each of the various single-Trp channel peptides can provide information relating to the peptide's solution structure. The acrylamide quenching data (k_q values; Table II, Figure 3B) implied that there were two segments of the channel peptide which were aqueous-exposed: the segment including 393–413 and a second segment including 431–443. Conversely, the N-terminal segment of the channel peptide (355–393), the small central portion (413–431), and the hydrophobic membrane anchor region (460–507) were largely inaccessible to the water-soluble

quencher acrylamide. Consistent with these results were those reported by Bishop *et al.* (1985), who showed that C-505 is buried within the channel peptide structure and that the peptide must be denatured with urea or guanidine hydrochloride in order to react thiol-specific reagents with the lone sulfhydryl. The purported membrane-anchoring segment A-474-I-508, located near the C-terminus, includes the single Cys residue of the channel peptide, and this peptide segment is believed to be buried in the soluble structure (Merrill *et al.*, 1990).

These findings are consistent with the current working model for the activation of the colicin E1 channel peptide to its insertion-competent state and are consistent with previous results (Merrill *et al.*, 1990). Activation caused a relatively small degree of unfolding of the channel peptide structure in solution. It involved an unfolding of the amino-terminal end and a small loosening at the COOH-terminal tail of the molecule. The largest changes in the peptide structure, as detected by the individual Trp residues in the various single-Trp peptides, occurred at positions 355, 367, 393, 413, and 443. The Trp-413 residue is the only site to report a significant decrease in quencher accessibility upon low-pH activation. The water-soluble quencher acrylamide detected a smaller unfolding of the peptide at residues 404, 431, 460, and 484. This latter region includes the purported membrane anchor segment (A-474-I-508), previously demonstrated to increase its degree of exposure to the aqueous solvent upon peptide activation (Merrill *et al.*, 1990).

We have deliberately avoided a discussion of our results in the context of the solved colicin A crystal structure (Parker *et al.*, 1992). Preliminary crystal structure analysis of the colicin E1 channel peptide structure indicated that there are significant differences between the colicin A and E1 channel peptide structures especially when considering the fine structural organization/orientation of individual residues. These results, along with the fact that the alignment of the two peptide sequences involves a large deletion in the colicin A sequence for optimal correlation of the two structures, indicate that structural comparisons between colicins E1 and A must be made with extreme caution (C. Stauffacher, personal communication). It is anticipated that the colicin E1 crystal structure will be shortly forthcoming and that a detailed comparison on a structural basis may be completed at that time.

Presently, we are studying the details of activation to the insertion-competent state by monitoring conformational changes occurring within the thermolytic peptide solution structure by fluorescence resonance energy transfer. In concert with these studies, we are also studying the general thermodynamics of thermolytic peptide unfolding by using the Trp residue as a reporter for specific peptide segments.

ACKNOWLEDGMENT

We thank Dr. William Cramer for kindly supplying us with the colicin E1 construct pSKE1$^-$ and the *E. coli* strain IT3661. We also thank Don Krajcarski for expert technical assistance in conducting the fluorescence lifetime experiments.

REFERENCES

Bishop, L. J., Bjes, E. S., Davidson, V. L., & Cramer, W. A. (1985) *J. Bacteriol. 164*, 237–244.

Brunden, K. R., Urantani, Y., & Cramer, W. A. (1984) *J. Biol. Chem. 259*, 7682–7687.

Bullock, J. O., Cohen, F. S., Dankert, J. R., & Cramer, W. A. (1983) *J. Biol. Chem. 258*, 9908–9912.

Burstein, E. A., Vedenkina, N. S., & Ivkova, M. N. (1973) *Photochem. Photobiol. 18*, 263–279.

Calhoun, D. B., Vanderkooi, J. M., Holtom, G. R., & Englander, S. W. (1986) *Proteins: Struct., Funct., Genet. 1*, 109–115.

Chen, Y. H., Yang, J. T., & Chau, K. H. (1974) *Biochemistry 13*, 3350–3359.

Cleveland, M. B., Slatin, S., Finkelstein, A., & Levinthal, C. (1983) *Proc. Natl. Acad. Sci. U.S.A. 80*, 3706–3710.

Creed, D. (1984) *Photochem. Photobiol. 39*, 537–562.

Davidson, V. L., Brunden, K. R., & Cramer, W. A. (1985) *Proc. Natl. Acad. Sci. U.S.A. 82*, 1386–1390.

Durbin, J., & Watson, G. S. (1971) *Biometrika 58*, 1.

Eftink, M. R., & Ghiron, C. A. (1981) *Anal. Biochem. 114*, 199–227.

Eftink, M. R., & Wasylewski, Z. (1989) *Biochemistry 28*, 382–391.

Goot, F. G., Gonzalez-Manas, J. M., Lakey, J. H., & Pattus, F. (1991) *Nature 354*, 408–410.

Gould, J. M., & Cramer, W. A. (1977) *J. Biol. Chem. 252*, 5491–5497.

Knutson, J. R., Beechem, J. M., & Brand, L. (1983) *Chem. Phys. Lett. 102*, 501–507.

Laws, W. R., & Contino, P. B. (1992) *Methods Enzymol. 210*, 448–463.

London, E. (1992) *Biochim. Biophys. Acta 1113*, 25–51.

Marquardt, D. W. (1963) *J. Soc. Ind. Appl. Math. 11*, 431–441.

Merrill, A. R., & Cramer, W. A. (1990) *Biochemistry 29*, 8529–8534.

Merrill, A. R., Cohen, F. S., & Cramer, W. A. (1990) *Biochemistry 29*, 5829–5836.

Moore, S., & Stein, W. H. (1963) *Methods Enzymol. 6*, 810–831.

Parker, C. A. (1968) in *Photoluminescence of Solutions*, p 220, Elsevier, New York.

Parker, M. W., Pattus, F., Tucker, A. D., & Tsernoglou, D. (1989) *Nature 337*, 93–96.

Parker, M. W., Postma, J. P. M., Pattus, F., Tucker, A. C., & Tsernoglou, D. (1992) *J. Mol. Biol. 224*, 639–657.

Permyakov, E. A. (1993) in *Luminescent Spectroscopy of Proteins*, p 48, CRC Press, Inc., London.

Peterson, A. A., & Cramer, W. A. (1987) *J. Membr. Biol. 99*, 197–204.

Ptitsyn, O. B. (1987) *J. Protein Chem. 6*, 273–293.

Randall, L. L., & Hardy, S. S. (1986) *Cell 46*, 921–928.

Rath, P., Bousche, O., Merrill, A. R., Cramer, W. A., & Rothchild, K. J. (1990) *Biophys. J. 59*, 516–522.

Schwartz, S. A., & Helsinki, D. R. (1971) *J. Biol. Chem. 246*, 6318–6327.

Shiver, J. W., Cramer, W. A., Cohen, F. S., Bishop, L. J., & de Jong, P. J. (1987) *J. Biol. Chem. 262*, 14273–14281.

Shiver, J. W., Cohen, F. S., Merrill, A. R., & Cramer, W. A. (1988) *Biochemistry 27*, 8421–8428.

Song, H. Y., Cohen, F. S., & Cramer, W. A. (1991) *J. Bacteriol. 173*, 2927–2934.

Willis, K. J., & Szabo, A. G. (1989) *Biochemistry 28*, 4902–4908.

Willis, K. J., & Szabo, A. G. (1992) *Biochemistry 31*, 8924–8931.

Wormald, M., Merrill, A. R., Cramer, W. A., & Williams, R. J. P. (1990) *Eur. J. Biochem. 191*, 155–165.

Yamada, M., Ebina, Y., Mayato, T., Nakazawa, T., & Nakazawa, A. (1982) *Proc. Natl. Acad. Sci. U.S.A. 79*, 2827–2831.

Zuker, M., Szabo, A. G., Bramall, L., Krajcarski, D. T., & Selinger, B. (1985) *Rev. Sci. Instrum. 56*, 14–22.